The damage signal IL-33 promotes a focal protective myeloid cell response to *Toxoplasma gondii* in the brain

Katherine M. Still*, Samantha J. Batista*, Jeremy A. Thompson*, Nikolas W. Hayes*, Carleigh O'Brien*, and Tajie H. Harris*

Affiliations: *Center for Brain Immunology and Glia, Department of Neuroscience, University of Virginia, Charlottesville, VA 22908

Corresponding Author and Lead Contact:

Tajie H. Harris, MR-4 Room 6148, 409 Lane Road, Charlottesville, VA 22908

Phone: 434-982-6916

Fax: 434-982-4380

Email: tajieharris@virginia.edu

This work was funded by National Institutes of Health grants R01NS091067 to T. H. H., T32GM008328 to K. M. S. and J. A. T., T32AI007046 to S. J. B., and T32AI007496 to C. A. O. and a University of Virginia School of Medicine R&D grant.

SUMMARY

An intact immune response is critical for survival of hosts chronically infected with *Toxoplasma gondii*. We observe clusters of macrophages surrounding replicating parasite in brain tissue, but the initial cues which instruct focal inflammatory reactions in the central nervous system (CNS) are not well understood. One potential mechanism of broad relevance is host cell damage. Here we find that IL-33, a nuclear alarmin, is critical for control of *T. gondii* parasites in the brain. IL-33 is expressed by oligodendrocytes and astrocytes during *T. gondii* infection, and a loss of nuclear IL-33 staining is observed in association with replicating *T. gondii* in infected mouse and human brain tissue, suggestive of IL-33 release. IL-33 signaling is required for induction of chemokines in astrocytes, including focal CCL2 production as visualized using CCL2-mCherry reporter mice. Bone marrow chimera experiments support the hypothesis that IL-33 could be acting directly on astrocytes, as the relevant IL-33-responding cell is radio-resistant. In alignment with CCL2 induction, IL-33 signaling is required for the infiltration of $CCR2^{+}$ myeloid cells that express anti-parasitic iNOS locally. These results expand our knowledge of alarmin signaling in the brain, an environment which is unique from the periphery and demonstrates the importance of a single damage signal in focal control of *T. gondii* infection in the CNS.

INTRODUCTION

Toxoplasma gondii is a eukaryotic parasite which encysts in the brain parenchyma of its hosts, including humans and mice[1-3]. Mortality from *T. gondii* infection is associated with conversion of the latent cyst form to fast-replicating parasites within CNS tissue. Increased prevalence of parasite replication has been documented in immunosuppressed patients undergoing transplant surgeries[4], HIV-AIDS patients[5-7], and in congenital infection[8]. Murine *T. gondii* infection features natural cyst formation with spontaneous reactivation and serves as a model for understanding how protective immune responses are generated in the brain[9,10].

A Th1-dominated immune response to *T. gondii* is essential for control of murine infection[1,2]. Depletion of T-cell derived IFN-γ during brain infection results in rapid mortality[11]. IFN-γ can stimulate anti-parasitic effector responses in macrophages, such as the production of reactive nitrogen species[2]. Macrophage-derived inducible nitric oxide synthase (iNOS) is effective at limiting parasite replication via direct toxicity and depletion of arginine *in vitro*[2,12]. iNOS is also vital to survival of chronic brain infection *in vivo*[13,14]. We find that blood-derived iNOS-expressing macrophages form foci around reactivated parasite during chronic infection. But how macrophages are recruited to the brain in response to *T. gondii*, and how they are instructed to reach specific sites within brain tissue where *T. gondii* is replicating is unclear.

During the acute, systemic stage of infection, the pattern recognition receptors TLR11 and TLR12 and Nod-like receptors NLRP1 and NLRP3 are involved in the activation of the immune system[15-18], but how and if *T. gondii* is recognized in the brain is not yet characterized. Sensing of damage-associated molecular patterns, however, may be a mechanism of broad relevance by which blood-derived myeloid cells are directed to the brain. Here we focus on a nuclear alarmin, IL-33, which acts as an amplifier of immune responses throughout the body[19-21]. Interestingly, *T. gondii*-infected mice deficient for the IL-33 receptor have been reported to exhibit brain pathology

and increased parasite burden, but the impact of IL-33 signaling on immune cell recruitment has not been addressed[22].

IL-33 is expressed in barrier tissues in the periphery, including the lung, gut, and skin, where it serves as a sentinel for barrier tissue disruption and is best known for its role in promoting type 2 immune responses during asthma, allergy, and helminth infection[19-21,23]. Because this nuclear protein does not contain a secretory signal peptide and does not require processing to be active, it is proposed to be released upon necrotic cell death[19,21,24]. Following its release, IL-33 acts on a heterodimer of the IL-1 receptor accessory protein (IL-1RacP) and its cognate receptor ST2 to initiate classical MyD88-NF-κB signaling which upregulates expression of chemokines and cytokines[20,21]. In the periphery, IL-33 can signal on a gamut of ST2-expressing cells of hematopoietic origin; those most commonly studied are type 2 innate lymphoid cells (ILC2s), mast cells, and regulatory T cells[20,21,25]. The ultimate effect of IL-33 signaling depends heavily on the responding cell type and environmental milieu and can serve either an inflammatory or homeostatic function[25].

IL-33 is more highly expressed in the brain and spinal cord than any other tissue[23], but its roles are only beginning to be described in the CNS. Nuclear IL-33 is expressed by astrocytes and myelinating oligodendrocytes in the healthy, adult mouse brain parenchyma[26,27]. Like IL-33 expression, IL-33 signaling during pathology in the brain likely differs from the periphery. ST2-expressing immune cells are physically separated from IL-33 expressing cells in the parenchyma by the BBB in a naïve state and would likely be unable to respond to initial insult[26,28-31]. Therefore, it is unknown if the generation of an immune response to brain pathology would necessitate IL-33 signaling on a brain-resident cell type. Nonetheless, IL-33 has been recently demonstrated to be beneficial in responding to insults affecting the parenchyma, including mouse models of Alzheimer's disease[32] and stroke[33], in which peripherally-administered IL-33 had beneficial effects on disease outcome. The mechanisms by which endogenous IL-33 generates immunity to various brain insults are still being defined.

Here we show that IL-33-expressing glia are lost in regions of replicating parasite within brain tissue. We report that IL-33 signals on a brain-resident responder to recruit blood-derived myeloid cells to the *T. gondii* infected brain. We find IL-33 impacts focal inflammation, inducing localized chemokine expression and iNOS production in macrophages. Although IL-33 has been predominantly connected with type 2 immune responses, we find that IL-33 signaling is required for limiting parasite burden in a heavily Th1-skewed environment. The mechanism outlined here may have relevance to human *T. gondii* infection and other neuropathological models featuring damage of IL-33-expressing glial cells.

RESULTS

Focal loss of IL-33-expressing glia is associated with replicating *T. gondii* in the brain

By four weeks post infection, *T. gondii* traffics to brain tissue of infected mice and exists in an intracellular cyst form which is slow growing[3,34](Figure 1A). Cysts are most prominent in the cerebral cortex[35], but can exist anywhere in the brain[9,36-38], and each cyst can contain hundreds of individual parasites[39]. We observe occasional cyst reactivation in which releases fast-replicating parasites are released into brain tissue (Figure 1A). Clusters of cells surround individual replicating parasites but not *T. gondii* cysts (Figure 1A). Therefore, we hypothesized that local damage signals are released in response to lytic *T. gondii* replication[40] which could mediate cellular recruitment. We focused on one candidate alarmin, IL-33, which is highly expressed in the CNS at baseline[23,26,27]. Consistent with IL-33 being a pre-stored alarmin, expression only mildly increases with infection (Figure S1A). While IL-33 expression is spread evenly throughout the naïve brain[26], we noticed focal loss of nuclear IL-33 staining in association with replicating parasite (Fig. 1B), suggesting potential alarmin release in these regions. In the *T. gondii* infected brain parenchyma, IL-33 is expressed by mature, $CC1^+$ mature oligodendrocytes and by astrocytes, the percentage of which varies by brain region (Figures 1C, 1D, 1E, and S1B). In gray matter, such as the cortex, 60% of IL-33 positive cells are oligodendrocytes and the remainder of the IL-33 expression is astrocytic (Figure 1E). But in white matter tracts such as the corpus callosum, nearly all of IL-33-expressing cells are oligodendrocytes (Figures 1D and 1E). Markers for these cell types are also absent at the center of inflammatory lesions, suggestive of glial cell death and possible local release of IL-33 in the *T. gondii*-infected brain parenchyma (Figure S1C).

We also detected IL-33 protein expression in astrocytes in healthy human brain tissue, but not in oligodendrocytes (Figures 1F and 1G). Innate recognition of *T. gondii* in the human brain

has not been described, due in part to the fact that TLRs 11 and 12 which recognize *T. gondii* acutely in mice are a pseudogene and nonexistent in humans, respectively[2,15,16,41]. In post-mortem brain tissue of a toxoplasmic encephalitis patient, we detected intact IL-33 staining in healthier regions of infected brain tissue, but IL-33 staining was absent from *T. gondii* lesions (Figure S1D). Collectively, these results indicate that IL-33 is expressed by glia in the *T. gondii* infected brain and is absent from lesions where *T. gondii* is replicating.

IL-33-ST2 signaling induces localized monocyte chemoattractant, CCL2

In order to interrogate the function of IL-33 in *T. gondii* infection, we considered its described role as an alarmin which recruits and activates immune cells[19-21]. Recruitment of immune cells to the brain is a highly-orchestrated process which requires upregulation of chemokine and adhesion factor expression. We probed whole brain homogenate by qRT-PCR from wildtype and IL-33R(ST2)-deficient mice for discrepancies in genes which could influence immune cell trafficking to the brain. $ST2^{-/-}$ mice exhibited defects in expression of the chemokines *ccl2*, *cxcl10*, and *cxcl1* compared with infected wildtype counterparts (Figure 2A), whereas expression of the adhesion factors *vcam* and *icam* were equivalent between genotypes (Figure 2A). Interestingly, *ccl2* and *cxcl10* expression has been attributed to astrocytes by *in situ* hybridization during *T. gondii* infection[42]. Although *cxcl1* has not been extensively studied in our system, it has been reported to be expressed in astrocytes during neuroinflammation[43]. We did not observe an effect, however, of IL-33 signaling on *cxcl9* expression– a chemokine which is made by PU.1-expressing cells, including microglia and macrophages, rather than astrocytes[44] (Fig. 2A). These results suggest that IL-33 may be acting directly on astrocytes to induce chemokine expression during *T. gondii* infection.

We next sought to visualize the localization of chemokine expression in relation to parasite replication within brain tissue. We focused on the chemokine with the greatest in expression between WT and $ST2^{-/-}$ mice, the monocyte chemoattractant CCL2. CCL2 expression is highly

upregulated in the brain following infection by approximately 100-fold (Fig. S2A). To gain a spatial understanding of CCL2 expression, we infected CCL2-mCherry reporter mice[45] and conducted immunofluorescence microscopy on chronically infected brain tissue. We observed CCL2 expression in "hotspots", which were present in brain lesions containing hallmarks of parasite reactivation, including destruction of brain-resident cells, absence of IL-33 staining, and accumulation of immune cells (Figures 2B-2E). Approximately 75% of CCL2-mCherry was expressed by astrocytes and 22% by Iba1^{+} macrophages, and 3% of cells did not co-stain with either of these markers (Figure S2B). CCL2-mCherry signal that could not be attributed to either cell type was present at the center of inflammatory lesions and could be derived from cellular debris or expressed by newly recruited monocytes which do not yet express the macrophage marker Iba1. Expression of CCL2 in inflammatory lesions led us to inquire whether CCL2 could be upregulated locally in response to IL-33. To this end, we crossed CCL2-mCherry reporter mice to ST2$^{-/-}$ mice to visualize CCL2 expression in the absence of IL-33 signaling. Sagittal brain section tile scans revealed that CCL2 foci in ST2$^{-/-}$ mice were much reduced in size compared with wildtype infected mice (Figures 2D and 2E). Multiple signals can likely induce CCL2 during infection, including other innate cytokines[46], but our data suggest that IL-33 is a major contributor to the induction of focal CCL2 expression in the *T. gondii* infected brain (Figures 2D and 2E).

Trafficking of blood-derived myeloid cells to the *T. gondii*-infected brain is dependent on IL-33-ST2 signaling

We next assessed the impact of IL-33-induced CCL2 expression on the recruitment of myeloid cells to the brain. Specifically, we were interested in the CCR2^{+} monocyte subset and macrophages derived from these cells. To distinguish myeloid cell subsets that enter the brain from the brain-resident microglia, we generated a microglia reporter mouse strain by crossing a CX3CR1-creERT2 mouse to an Ai6 (Zsgreen) cre-reporter mouse. Mice were given tamoxifen at

weaning, labeling most myeloid cells, including microglia[47,48]. We waited four weeks post-tamoxifen treatment to allow for peripheral turnover of Zsgreen-expressing cells while microglia remained labeled. With these mice, we were able to visualize a robust increase in cell number of unlabeled (Zsgreen-), $CD45^{hi}$, $CD11b^{+}$ infiltrating myeloid cells in the brain during chronic *T. gondii* infection (Figure 3A). Blood-derived macrophages were not only present in the brain during infection (Figure 3B), but also clustered with high fidelity around replicating parasite (Figure S3A), as distinguished from microglia in brain tissue sections using the microglia reporter mouse. While a small percentage of microglia upregulate CD45 upon infection, we found that over 90% of $Zsgreen^{+}$ microglia were captured by a $CD45^{int}$ gate by flow cytometry (Fig. S3B). Therefore, we used CD45 expression to distinguish microglia from infiltrating myeloid cells in future flow cytometry experiments.

Recruitment of myeloid cells to the *T. gondii*-infected brain was dependent on IL-33-ST2 signaling. The frequency and number of engrafted myeloid cells denoted by $CD45^{hi}$ $CD11b^{+}$ cells were decreased in infected $ST2^{-/-}$ brains compared with controls by flow cytometry (Figures 3C and 3D), while $CD45^{int}$ $CD11b^{+}$ microglia numbers were unchanged (Figure 3D). Importantly, this phenomenon was brain-specific. $ST2^{-/-}$ spleens contained higher numbers of $CD11b^{+}$ cells than controls, which was not evident at baseline, supportive of a brain recruitment defect (Figures S3C, S3D). Numbers of myeloid cells were also comparable in ST2-deficient and wildtype mice during acute infection (Figure S3E and S3F). To confirm that myeloid cells recruited to the brain were monocyte-derived and capable of responding to CCL2, we crossed $ST2^{-/-}$ mice to a CCR2-RFP reporter mouse. At four weeks post infection, $ST2^{-/-}$ mice displayed a marked decrease in $CCR2^{+}$ cell infiltration (Figures 3E, 3F, and 3G) by immunohistochemistry.

IL-33 signals on a radio-resistant responder to recruit myeloid cells to the brain

Given that a wide range of cells have been reported to express ST2[19,21,25], we were curious which ST2-expressing cell type was responsible for mediating IL-33-dependent recruitment of

myeloid cells to the brain. We detected ST2 on innate lymphoid cells (ILC2s) in the brain, as well as regulatory T cells (Tregs) (Figures S4A and S4B). But it is unclear if ILC2s would be relevant to monocyte recruitment during a Th1-dominated infection, and Tregs are spatially restricted from the parenchyma even after *T. gondii* infection[31]. ST2 mRNA has also been reported in microglia and astrocytes[49]. Therefore, we performed a bone marrow chimera to determine if IL-33 signals on a radio-sensitive or a radio-resistant cell type to recruit myeloid cells to the brain. Briefly, we lethally irradiated wildtype and $ST2^{-/-}$ mice, then reconstituted these mice with bone marrow from wildtype donors or $ST2^{-/-}$ donors, and allowed 6 weeks for reconstitution before infection (Figure 3H). We found that ST2-deficient recipients which received wildtype bone marrow resembled ST2-deficient mice which received ST2-deficient bone marrow, suggesting that a hematopoietic source of ST2 is irrelevant for IL-33-mediated recruitment of infiltrating myeloid cells to the brain (Figure 3I). These results are consistent with our hypothesis that IL-33 acts directly on astrocytes to induce CCL2 expression and recruit monocyte-derived myeloid cells to the brain.

IL-33-ST2 signaling is required for engrafted myeloid cell-derived iNOS expression

We next probed further into the blood-derived myeloid compartment to assess the anti-parasitic capacity of these cells in the absence of IL-33 signaling. One of the most powerful mechanisms myeloid cells can employ to limit parasite is the production of NO by inducible nitric oxide synthase (iNOS)[2,13,14]. We assessed which cells expressed iNOS in the brain by flow cytometry using the microglia reporter mouse. All of the iNOS in the infected brain can be attributed to $CD11b^{+}$ myeloid cells, only a tenth of which is produced by microglia (Figures 4A and 4B). Peripherally-derived macrophages far outnumber microglia and the frequency of iNOS expressing cells within the microglia population was also much lower than that of infiltrating myeloid cells (Figure 4A).

We found IL-33-ST2 signaling to be required for adequate iNOS expression by peripherally-derived macrophages (Figures 4C and 4D). Beyond a macrophage recruitment

defect, iNOS positive infiltrating myeloid cells were reduced in frequency (Figure 4C), suggesting that of the cells that reach the brain, fewer are anti-parasitic without IL-33 signaling. IL-33 is not likely to influence iNOS production in infiltrating macrophages directly, as we did not detect ST2 in these cells (Figure S4C). Alternatively, we propose that IL-33-induced chemokine directs infiltrated macrophages to inflammatory lesions where local signals that can upregulate iNOS are concentrated. Indeed, iNOS expression by macrophages in the *T. gondii*-infected brain is localized in clusters, and the size of these foci are dependent on IL-33 signaling (Figures 4E and 4F). One signal which is required for iNOS expression is IFN-γ, which acts through STAT1[1,2]. We observe reduced foci of phosphorylated STAT1-positive macrophages in tissue sections in the absence of IL-33 signaling (Figure S4D). These results emphasize that not only are fewer macrophages recruited to the *T. gondii* infected brain in the absence of IL-33 signaling, but fewer are instructed by IFN-γ to make iNOS within inflammatory lesions.

ST2$^{-/-}$ mice have deficient CD4^{+} T cell responses

IFN-γ is almost exclusively T cell-derived in the *T. gondii*-infected brain (Figure S5A). Reduced phosphorylated-STAT1 and IFN-γ–inducible iNOS expression in inflammatory foci of infected ST2$^{-/-}$ mice pointed to a reduction in T cell-derived IFN-γ near replicating parasites. T cells are indeed present in lesions containing replicating *T. gondii*, but cluster less densely than macrophages (Figure S5B). When we assessed T cell numbers by flow cytometry in ST2 deficient mice, we observed a decrease in CD4^{+}, but not CD8^{+} T cells (Figure 5A). CD4^{+} T cells displayed reduced proliferation, *T. gondii*-tetramer specificity, and cytokine secretion in ST2$^{-/-}$ mice (Figures 5B and 5C), whereas CD8^{+} function was unaffected (Figures S5C and S5D). These results could potentially be explained by the decrease of MHCII-expressing cells in the brains of ST2$^{-/-}$ mice, which may provide less opportunity for local CD4^{+} T cell activation (Figure 5D). Importantly, T cell responses were unaffected in the periphery and during the acute stage of infection in ST2$^{-/-}$ mice

(Figures S5E-G). These results highlight the compounding effect of ST2 deficiency in anti-parasitic capacity displayed by both myeloid cells and T cells during chronic *T. gondii* infection.

IL-33-ST2 signaling is required for control of brain parasite burden

The ultimate consequence of the absence of IL-33-ST2 signaling is an increase in brain parasite burden (Figures 6A, 6B). Tissue cysts observed by H & E staining of infected brain tissue were present in clusters in $ST2^{-/-}$ mice, a phenomenon which does not occur frequently in wildtype mice (Figure 6A). We propose that in $ST2^{-/-}$ mice, parasite reactivation events are not properly controlled, resulting in increased opportunity for parasite to encyst in neighboring cells. Importantly, parasite was cleared from peripheral tissues in acute stages of infection in ST2-deficient mice (data not shown). While parasite burden does increase, $ST2^{-/-}$ mice do not succumb to infection, which implies that there are additional signals that mobilize and shape the protective immune response to chronic *Toxoplasma gondii* infection. In any case, IL-33 plays a non-redundant role and contributes significantly to the control of chronic *T. gondii* infection.

DISCUSSION

Instructing immune cells to enter the brain and reach particular sites within brain tissue requires fine-tuned orchestration[50-52]. Chemokines can impact behavior and interaction of immune cells within the brain parenchyma[52], but the signals which precede chemokine production, in our system and in many others, are often not understood. Our results pinpoint a damage-associated cue, IL-33, which induces localized production of monocyte chemoattractant in the *T. gondii*-infected brain. IL-33 is necessary for the congregation of nitric-oxide-producing myeloid cells within the parenchyma and, consequently, is necessary to limit parasite burden.

There are several interesting aspects of IL-33 expression which lend themselves to further study. Each tissue in the body contains resident cells that detect perturbations and communicate to peripheral immune cells[53]. In both the naïve and *T. gondii*-infected adult brain parenchyma, IL-33 is not expressed by all brain-resident cells, but rather is restricted to myelinating oligodendrocytes and astrocytes. This is in stark contrast to HMGB1, which is expressed ubiquitously in the brain[30]. Common intracellular contents which can also signal damage, such as ATP and uric acid, are also housed in nearly all cell types. We find that the majority of IL-33 expression in the infected, adult mouse brain is derived from oligodendrocytes, specifically, mature myelinating oligodendrocytes, implicating these cells as sentinels of tissue damage. IL-33 expression by mature oligodendrocytes, rather than oligodendrocyte progenitors is consistent with the observation of IL-33 expression in terminally differentiated cells throughout the rest of the body, including barrier cells and cardiomyocytes[20,54,55]. Oligodendrocytes are uniquely susceptible to several initiators of cell death, including oxidative stress, sphingolipid-derived ceramide signaling, and glutamate excitotoxicity[56]. IL-33 may be involved in any brain insult associated with oligodendrocyte death, including even normal aging, where excitotoxicity to oligodendrocytes has been reported[56,57].

We have identified IL-33 expression by astrocytes in the healthy human brain, but not by oligodendrocytes. Discrepancies by which brain cells release IL-33 between humans and mice is

of translational interest and is a topic for further study. We posit that IL-33 signaling has relevance to human *T. gondii* infection, as we documented a loss of IL-33 staining in regions of parasite deposition within the brain of a human toxoplasmic encephalitis patient. Recognition of damage caused by a pathogen may be a more broadly relevant mechanism for engendering an immune response than recognition of the pathogen itself through germline encoded receptors. Alarmin signaling would allow more species, including humans, to detect *Toxoplasma*, since the murine-specific TLRs 11 and 12 which recognize a *T. gondii* cytoskeletal protein are a pseudogene or nonexistent in humans, respectively[15,16,41,58,59]. IL-33 signaling could result in similar consequences as TLR signaling described in response to *T. gondii* in mice, since both pathways converge on MyD88 and NF-κB[30].

We have established that IL-33 acts on a radio-resistant responder to recruit immune cells to the *T. gondii*-infected brain, although IL-33 has been most commonly reported to signal on immune cells in the periphery[19-21,25]. For reasons that are unclear, ST2 expression has not been convincingly shown on the protein level on any brain resident cell types, but IL-33 ST2 signaling on glia has been suggested in other studies focused on the CNS. In the retina, IL-33 is released from, and acts on, Müller cells in an autocrine fashion in response to phototoxic stress[55]. In the brain, ST2 mRNA has been detected in both astrocytes and microglia[49]. During brain development, specific deletion of ST2 in microglia led to disrupted synapse engulfment[27]. There is also a suggestion that the relevant ST2-bearing cell can rapidly change with insult. A prior study demonstrated that a $CD11b^{+}$ fraction from uninjured spinal cord was ST2 positive, whereas the majority of ST2 expression from contused spinal cord glia was CD11b-negative[26]. Indeed, we observe by RNA-seq that microglia express detectable ST2 at baseline, but expression decreases 10-fold with infection (unpublished observations). The current study implicates astrocytes as a potential responder to IL-33 during infection. Therefore, our study and others support a glia-glia communication for IL-33 signaling in the CNS.

The most well-described function of IL-33 is the potentiation of type 2 immune responses, characterized by secretion of the cytokines IL-4, IL-5, and IL-13, and the involvement of type 2 innate lymphoid cells and alternatively activated macrophages[19-21,25]. But the definition of IL-33 signaling is broadening; IL-33 now has described roles for inducing a Th1-skewed immune response[60,61], and roles in tissue homeostasis[25]. Our work furthers the idea that the outcome of IL-33 signaling is highly dependent on the inflammatory environment. We find that IL-33 plays a role in potentiating the type 1-skewed response necessary for controlling *T. gondii* in the brain. We demonstrate that IL-33 is required for myeloid cell-derived nitric oxide production in inflammatory lesions. It is unclear how IL-33 mediates this effect, since iNOS-positive cells in our system do not express ST2. We suggest that IL-33 recruits cells via astrocyte-derived chemokine to areas in the brain which contain signals to induce iNOS expression. One of these is likely IFN-γ, but it is possible that other alarmins, or recognition of the parasite itself, could influence anti-parasitic capacity in inflammatory lesions. IL-33 signaling also did not seem to impact the brain vasculature, but other alarmins may activate the vasculature to promote monocyte cell entry, illustrating the complex process necessary for recruitment of cells to specific regions of the CNS.

Ultimately, our results demonstrate the importance of one alarmin in controlling a pathogen which infects the brain parenchyma. IL-33 signaling is required for local immune responses generated during *T. gondii* infection of the immunologically-unique CNS. Since ST2$^{-/-}$ mice do not succumb to infection, additional mechanisms are likely at play during chronic *T. gondii* infection, including signaling by other alarmins, such as ATP, HMGB1, S100 proteins, and IL-1α.

ACKNOWLEDGEMENTS

The authors would like to acknowledge members of the Harris lab and center for Brain Immunology and Glia (BIG) for their valuable input during the development of this work. We thank Sachin P. Gadani and Kenneth S. Tung for the discussions regarding IL-33. We thank Marieke K. Jones for her guidance with statistical analysis and coding. We would like to acknowledge the support we received from core facilities at the University of Virginia, including the Biorepository and Tissue Research Facility, the Flow Cytometry Core, and the Research Histology Core.

CONTRIBUTIONS

Conceptualization, K. M. S. and T. H. H.; Investigation, K. M. S., S. J. B., J. A. T., N. W. H., and C. A. O.; Writing—Original Draft, K. M. S.; Writing—Reviewing and Editing, K. M. S., S. J. B., N. W. H., C. A. O., and T. H. H.; Funding Acquisition, T. H. H.; Supervision, T. H. H.

DECLARATION OF INTERESTS

The authors declare no competing interests.

REFERENCES

1 Hunter, C. A. & Sibley, L. D. Modulation of innate immunity by Toxoplasma gondii virulence effectors. *Nat Rev Microbiol* **10**, 766-778, doi:10.1038/nrmicro2858 (2012).

2 Yarovinsky, F. Innate immunity to Toxoplasma gondii infection. *Nat Rev Immunol* **14**, 109-121, doi:10.1038/nri3598 (2014).

3 Dubey, J. P., Lindsay, D. S. & Speer, C. A. Structures of Toxoplasma gondii tachyzoites, bradyzoites, and sporozoites and biology and development of tissue cysts. *Clin Microbiol Rev* **11**, 267-299 (1998).

4 Slavin, M. A., Meyers, J. D., Remington, J. S. & Hackman, R. C. Toxoplasma gondii infection in marrow transplant recipients: a 20 year experience. *Bone Marrow Transplant* **13**, 549-557 (1994).

5 Luft, B. J. & Remington, J. S. Toxoplasmic encephalitis in AIDS. *Clin Infect Dis* **15**, 211-222 (1992).

6 Luft, B. J. & Remington, J. S. AIDS commentary. Toxoplasmic encephalitis. *J Infect Dis* **157**, 1-6 (1988).

7 Hunter, C. A. & Remington, J. S. Immunopathogenesis of toxoplasmic encephalitis. *J Infect Dis* **170**, 1057-1067 (1994).

8 Frenkel, J. K. Congenital toxoplasmosis: prevention or palliation? *Am J Obstet Gynecol* **141**, 359-361 (1981).

9 Ferguson, D. J., Graham, D. I. & Hutchison, W. M. Pathological changes in the brains of mice infected with Toxoplasma gondii: a histological, immunocytochemical and ultrastructural study. *Int J Exp Pathol* **72**, 463-474 (1991).

10 Waree, P., Ferguson, D. J., Pongponratn, E., Chaisri, U. & Sukthana, Y. Immunohistochemical study of acute and chronic toxoplasmosis in experimentally infected mice. *Southeast Asian J Trop Med Public Health* **38**, 223-231 (2007).

11 Gazzinelli, R., Xu, Y., Hieny, S., Cheever, A. & Sher, A. Simultaneous depletion of CD4+ and CD8+ T lymphocytes is required to reactivate chronic infection with Toxoplasma gondii. *J Immunol* **149**, 175-180 (1992).

12 Fox, B. A., Gigley, J. P. & Bzik, D. J. Toxoplasma gondii lacks the enzymes required for de novo arginine biosynthesis and arginine starvation triggers cyst formation. *Int J Parasitol* **34**, 323-331, doi:10.1016/j.ijpara.2003.12.001 (2004).

13 Scharton-Kersten, T. M., Yap, G., Magram, J. & Sher, A. Inducible nitric oxide is essential for host control of persistent but not acute infection with the intracellular pathogen Toxoplasma gondii. *J Exp Med* **185**, 1261-1273 (1997).

14 Schluter, D. *et al.* Inhibition of inducible nitric oxide synthase exacerbates chronic cerebral toxoplasmosis in Toxoplasma gondii-susceptible C57BL/6 mice but does not reactivate the latent disease in T. gondii-resistant BALB/c mice. *J Immunol* **162**, 3512-3518 (1999).

15 Yarovinsky, F. *et al.* TLR11 activation of dendritic cells by a protozoan profilin-like protein. *Science* **308**, 1626-1629, doi:10.1126/science.1109893 (2005).

16 Koblansky, A. A. *et al.* Recognition of profilin by Toll-like receptor 12 is critical for host resistance to Toxoplasma gondii. *Immunity* **38**, 119-130, doi:10.1016/j.immuni.2012.09.016 (2013).

17 Gorfu, G. *et al.* Dual role for inflammasome sensors NLRP1 and NLRP3 in murine resistance to Toxoplasma gondii. *MBio* **5**, doi:10.1128/mBio.01117-13 (2014).

18 Ewald, S. E., Chavarria-Smith, J. & Boothroyd, J. C. NLRP1 is an inflammasome sensor for Toxoplasma gondii. *Infect Immun* **82**, 460-468, doi:10.1128/IAI.01170-13 (2014).

19 Martin, N. T. & Martin, M. U. Interleukin 33 is a guardian of barriers and a local alarmin. *Nat Immunol* **17**, 122-131, doi:10.1038/ni.3370 (2016).

20 Liew, F. Y., Girard, J. P. & Turnquist, H. R. Interleukin-33 in health and disease. *Nat Rev Immunol* **16**, 676-689, doi:10.1038/nri.2016.95 (2016).

21 Liew, F. Y., Pitman, N. I. & McInnes, I. B. Disease-associated functions of IL-33: the new kid in the IL-1 family. *Nat Rev Immunol* **10**, 103-110, doi:10.1038/nri2692 (2010).

22 Jones, L. A. *et al.* IL-33 receptor (T1/ST2) signalling is necessary to prevent the development of encephalitis in mice infected with Toxoplasma gondii. *Eur J Immunol* **40**, 426-436, doi:10.1002/eji.200939705 (2010).

23 Schmitz, J. *et al.* IL-33, an interleukin-1-like cytokine that signals via the IL-1 receptor-related protein ST2 and induces T helper type 2-associated cytokines. *Immunity* **23**, 479-490, doi:10.1016/j.immuni.2005.09.015 (2005).

24 Cayrol, C. & Girard, J. P. The IL-1-like cytokine IL-33 is inactivated after maturation by caspase-1. *Proc Natl Acad Sci U S A* **106**, 9021-9026, doi:10.1073/pnas.0812690106 (2009).

25 Molofsky, A. B., Savage, A. K. & Locksley, R. M. Interleukin-33 in Tissue Homeostasis, Injury, and Inflammation. *Immunity* **42**, 1005-1019, doi:10.1016/j.immuni.2015.06.006 (2015).

26 Gadani, S. P., Walsh, J. T., Smirnov, I., Zheng, J. & Kipnis, J. The glia-derived alarmin IL-33 orchestrates the immune response and promotes recovery following CNS injury. *Neuron* **85**, 703-709, doi:10.1016/j.neuron.2015.01.013 (2015).

27 Vainchtein, I. D. *et al.* Astrocyte-derived interleukin-33 promotes microglial synapse engulfment and neural circuit development. *Science* **359**, 1269-1273, doi:10.1126/science.aal3589 (2018).

28 Louveau, A., Harris, T. H. & Kipnis, J. Revisiting the Mechanisms of CNS Immune Privilege. *Trends Immunol* **36**, 569-577, doi:10.1016/j.it.2015.08.006 (2015).

29 Gadani, S. P., Smirnov, I., Smith, A. T., Overall, C. C. & Kipnis, J. Characterization of meningeal type 2 innate lymphocytes and their response to CNS injury. *J Exp Med* **214**, 285-296, doi:10.1084/jem.20161982 (2017).

30 Gadani, S. P., Walsh, J. T., Lukens, J. R. & Kipnis, J. Dealing with Danger in the CNS: The Response of the Immune System to Injury. *Neuron* **87**, 47-62, doi:10.1016/j.neuron.2015.05.019 (2015).

31 O'Brien, C. A. *et al.* CD11c-Expressing Cells Affect Regulatory T Cell Behavior in the Meninges during Central Nervous System Infection. *J Immunol* **198**, 4054-4061, doi:10.4049/jimmunol.1601581 (2017).

32 Fu, A. K. *et al.* IL-33 ameliorates Alzheimer's disease-like pathology and cognitive decline. *Proc Natl Acad Sci U S A* **113**, E2705-2713, doi:10.1073/pnas.1604032113 (2016).

33 Luo, H., Higuchi, K., Matsumoto, K. & Mori, M. An interleukin-33 gene polymorphism is a modifier for eosinophilia in rats. *Genes Immun* **14**, 192-197, doi:10.1038/gene.2013.7 (2013).

34 Saeij, J. P., Boyle, J. P., Grigg, M. E., Arrizabalaga, G. & Boothroyd, J. C. Bioluminescence imaging of Toxoplasma gondii infection in living mice reveals dramatic differences between strains. *Infect Immun* **73**, 695-702, doi:10.1128/IAI.73.2.695-702.2005 (2005).

35 Cabral, C. M. *et al.* Neurons are the Primary Target Cell for the Brain-Tropic Intracellular Parasite Toxoplasma gondii. *PLoS Pathog* **12**, e1005447, doi:10.1371/journal.ppat.1005447 (2016).

36 Di Cristina, M. *et al.* Temporal and spatial distribution of Toxoplasma gondii differentiation into Bradyzoites and tissue cyst formation in vivo. *Infect Immun* **76**, 3491-3501, doi:10.1128/IAI.00254-08 (2008).

37 Kittas, S., Kittas, C., Paizi-Biza, P. & Henry, L. A histological and immunohistochemical study of the changes induced in the brains of white mice by infection with Toxoplasma gondii. *Br J Exp Pathol* **65**, 67-74 (1984).

38 Berenreiterova, M., Flegr, J., Kubena, A. A. & Nemec, P. The distribution of Toxoplasma gondii cysts in the brain of a mouse with latent toxoplasmosis: implications for the

behavioral manipulation hypothesis. *PLoS One* **6**, e28925, doi:10.1371/journal.pone.0028925 (2011).

39 Hill, D. E., Chirukandoth, S. & Dubey, J. P. Biology and epidemiology of Toxoplasma gondii in man and animals. *Anim Health Res Rev* **6**, 41-61 (2005).

40 Black, M. W. & Boothroyd, J. C. Lytic cycle of Toxoplasma gondii. *Microbiol Mol Biol Rev* **64**, 607-623 (2000).

41 Roach, J. C. *et al.* The evolution of vertebrate Toll-like receptors. *Proc Natl Acad Sci U S A* **102**, 9577-9582, doi:10.1073/pnas.0502272102 (2005).

42 Strack, A., Asensio, V. C., Campbell, I. L., Schluter, D. & Deckert, M. Chemokines are differentially expressed by astrocytes, microglia and inflammatory leukocytes in Toxoplasma encephalitis and critically regulated by interferon-gamma. *Acta Neuropathol* **103**, 458-468, doi:10.1007/s00401-001-0491-7 (2002).

43 Kang, Z. *et al.* Act1 mediates IL-17-induced EAE pathogenesis selectively in NG2+ glial cells. *Nat Neurosci* **16**, 1401-1408, doi:10.1038/nn.3505 (2013).

44 Ellis, S. L. *et al.* The cell-specific induction of CXC chemokine ligand 9 mediated by IFN-gamma in microglia of the central nervous system is determined by the myeloid transcription factor PU.1. *J Immunol* **185**, 1864-1877, doi:10.4049/jimmunol.1000900 (2010).

45 Shi, C. *et al.* Bone marrow mesenchymal stem and progenitor cells induce monocyte emigration in response to circulating toll-like receptor ligands. *Immunity* **34**, 590-601, doi:10.1016/j.immuni.2011.02.016 (2011).

46 Shi, C. & Pamer, E. G. Monocyte recruitment during infection and inflammation. *Nat Rev Immunol* **11**, 762-774, doi:10.1038/nri3070 (2011).

47 Yona, S. *et al.* Fate mapping reveals origins and dynamics of monocytes and tissue macrophages under homeostasis. *Immunity* **38**, 79-91, doi:10.1016/j.immuni.2012.12.001 (2013).

48 Madisen, L. *et al.* A robust and high-throughput Cre reporting and characterization system for the whole mouse brain. *Nat Neurosci* **13**, 133-140, doi:10.1038/nn.2467 (2010).

49 Yasuoka, S. *et al.* Production and functions of IL-33 in the central nervous system. *Brain Res* **1385**, 8-17, doi:10.1016/j.brainres.2011.02.045 (2011).

50 Sa, Q. *et al.* VCAM-1/alpha4beta1 integrin interaction is crucial for prompt recruitment of immune T cells into the brain during the early stage of reactivation of chronic infection with Toxoplasma gondii to prevent toxoplasmic encephalitis. *Infect Immun* **82**, 2826-2839, doi:10.1128/IAI.01494-13 (2014).

51 Wilson, E. H., Weninger, W. & Hunter, C. A. Trafficking of immune cells in the central nervous system. *J Clin Invest* **120**, 1368-1379, doi:10.1172/JCI41911 (2010).

52 Harris, T. H. *et al.* Generalized Levy walks and the role of chemokines in migration of effector CD8+ T cells. *Nature* **486**, 545-548, doi:10.1038/nature11098 (2012).

53 von Moltke, J. & Pepper, M. Sentinels of the Type 2 Immune Response. *Trends Immunol* **39**, 99-111, doi:10.1016/j.it.2017.10.004 (2018).

54 Chen, W. Y., Hong, J., Gannon, J., Kakkar, R. & Lee, R. T. Myocardial pressure overload induces systemic inflammation through endothelial cell IL-33. *Proc Natl Acad Sci U S A* **112**, 7249-7254, doi:10.1073/pnas.1424236112 (2015).

55 Xi, H. *et al.* IL-33 amplifies an innate immune response in the degenerating retina. *J Exp Med* **213**, 189-207, doi:10.1084/jem.20150894 (2016).

56 McTigue, D. M. & Tripathi, R. B. The life, death, and replacement of oligodendrocytes in the adult CNS. *J Neurochem* **107**, 1-19, doi:10.1111/j.1471-4159.2008.05570.x (2008).

57 Mattson, M. P. Excitotoxic and excitoprotective mechanisms: abundant targets for the prevention and treatment of neurodegenerative disorders. *Neuromolecular Med* **3**, 65-94, doi:10.1385/NMM:3:2:65 (2003).

58 Andrade, W. A. *et al.* Combined action of nucleic acid-sensing Toll-like receptors and TLR11/TLR12 heterodimers imparts resistance to Toxoplasma gondii in mice. *Cell Host Microbe* **13**, 42-53, doi:10.1016/j.chom.2012.12.003 (2013).

59 Gazzinelli, R. T., Mendonca-Neto, R., Lilue, J., Howard, J. & Sher, A. Innate resistance against Toxoplasma gondii: an evolutionary tale of mice, cats, and men. *Cell Host Microbe* **15**, 132-138, doi:10.1016/j.chom.2014.01.004 (2014).

60 Baumann, C. *et al.* T-bet- and STAT4-dependent IL-33 receptor expression directly promotes antiviral Th1 cell responses. *Proc Natl Acad Sci U S A* **112**, 4056-4061, doi:10.1073/pnas.1418549112 (2015).

61 Bonilla, W. V. *et al.* The alarmin interleukin-33 drives protective antiviral CD8(+) T cell responses. *Science* **335**, 984-989, doi:10.1126/science.1215418 (2012).

FIGURES

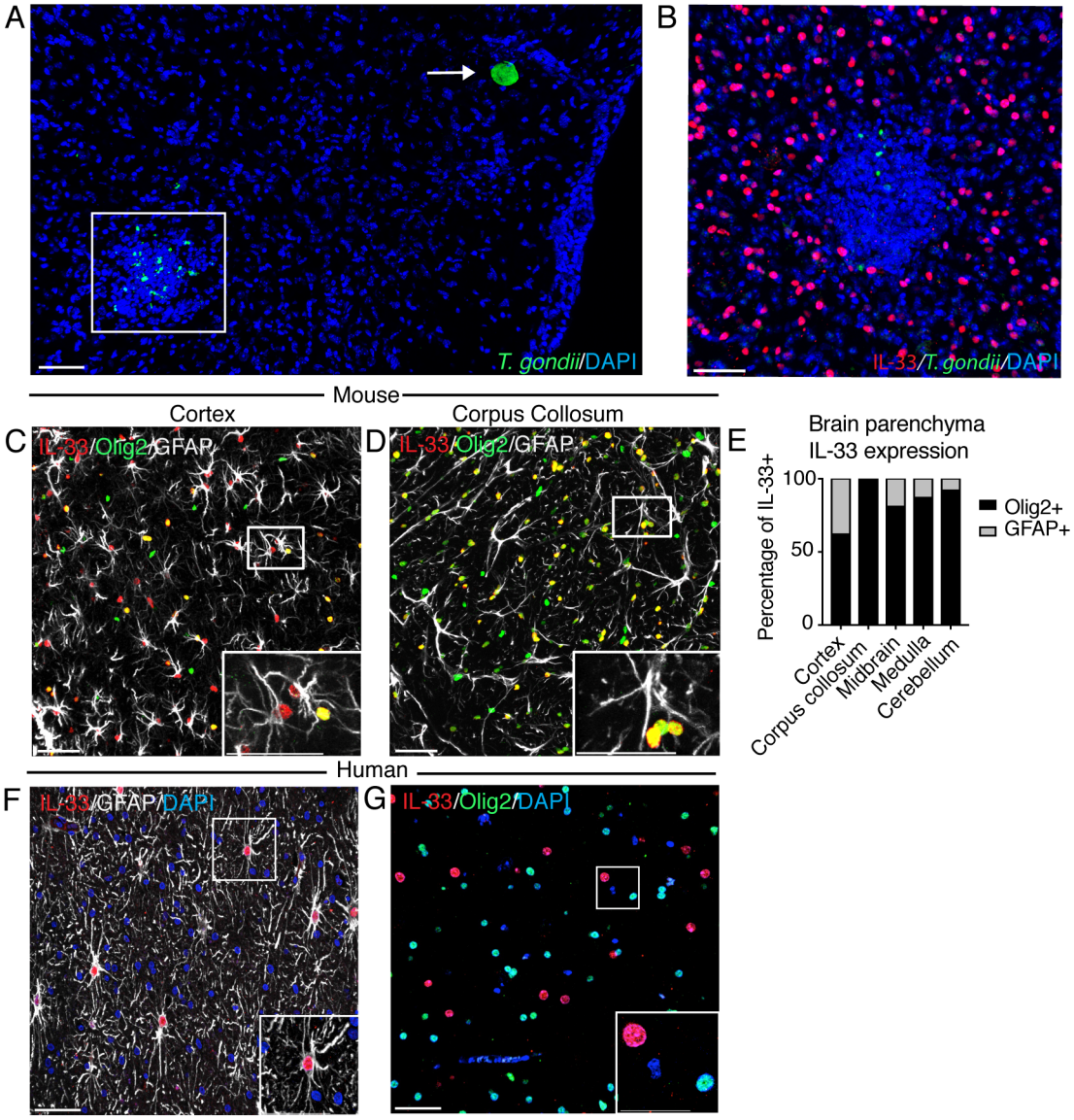

Figure 1. Focal loss of IL-33 is associated with replicating *T. gondii* in the brain

(A) Immunofluorescence staining of chronically infected mouse cortex for *T. gondii* (green) - detected in cyst form (arrow) and its reactivated replicating form (box), DAPI staining was used to detect nuclei (blue)

(B) Immunofluorescence staining of an inflammatory lesion for IL-33 (red) and *T. gondii* (green) in chronically infected mouse brain tissue – DAPI staining was used to detect nuclei (blue)

(C-D) Representative brain region immunofluorescence staining for IL-33 (red), $Olig2^+$ oligodendrocytes (green), and $GFAP^+$ astrocytes (white) in chronically infected mouse gray matter (cortex) (C) and white matter (corpus collosum) (D)

(E) Percentage of $IL\text{-}33^+$ cells which are $Olig2^+$ oligodendrocytes or $GFAP^+$ astrocytes by brain region, n=>30 cells per brain region, representative of 2 independent experiments

(F-G) Immunofluorescence staining of healthy human temporal lobe brain tissue for IL-33 (red), colocalized with $GFAP^+$ astrocytes (white) (F), and not co-localized with $Olig2^+$ oligodendrocytes (green) (G), (n=3), scale bars = 50μm

See also Figure S1

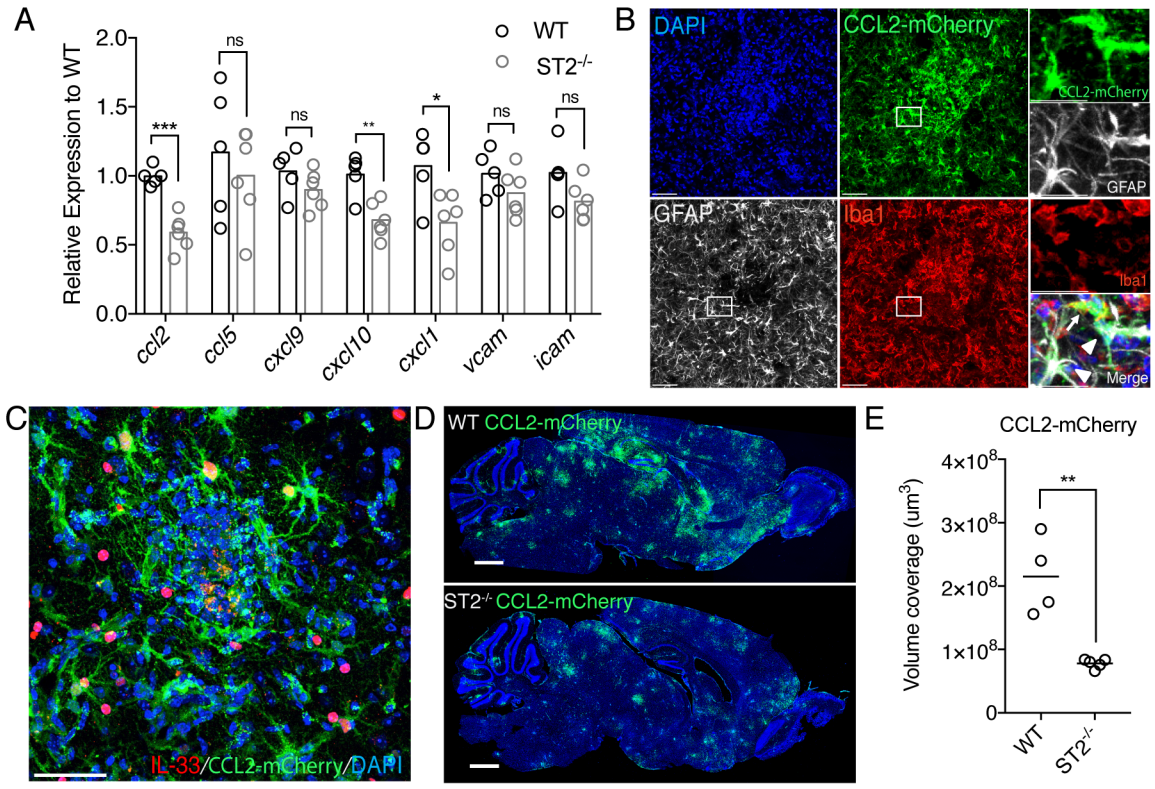

Figure 2. IL-33-ST2 signaling induces localized monocyte chemoattractant, CCL2

(A) Quantitative real time PCR was performed on RNA isolated from whole brain homogenate of chronically infected wildtype and ST2$^{-/-}$ mice, (n=5-6 per group, Student's t-test)

(B) Immunofluorescence staining of an inflammatory lesion in chronically infected CCL2-mCherry reporter brain tissue for mCherry (green), GFAP^{+} astrocytes (white), and Iba1^{+} macrophages (red) – DAPI staining was used to detect nuclei (blue), scale bar = 50μm. Insets depict co-stained CCL2-mCherry with GFAP^{+} astrocytes and an Iba1^{+} macrophage, scale bar = 20μm

(C) Immunofluorescence staining of an inflammatory lesion in chronically infected mouse brain tissue for IL-33 (red) and mCherry (green) – DAPI was used to detect nuclei (blue), scale bar = 50μm

555 (D) Representative tile scans of chronically infected wildtype and ST2$^{-/-}$ CCL2-mCherry reporter
556 mice. Sagittal brain slices were stained for mCherry and DAPI staining was used to detect nuclei
557 (blue), scale bar = 2000 µm
558 (E) Quantification of (D) by volume coverage of CCL2-mCherry voxels in sagittal brain sections
559 using Imaris software, (n=4-5 per group, Student's t-test, data points are representative of 3
560 averaged brain sections per mouse, overall data is representative of 3 independent experiments)
561 ns=p>0.05, *=p<0.05, **=p<0.01, ***=p<0.001
562 See also Figure S2.
563
564
565

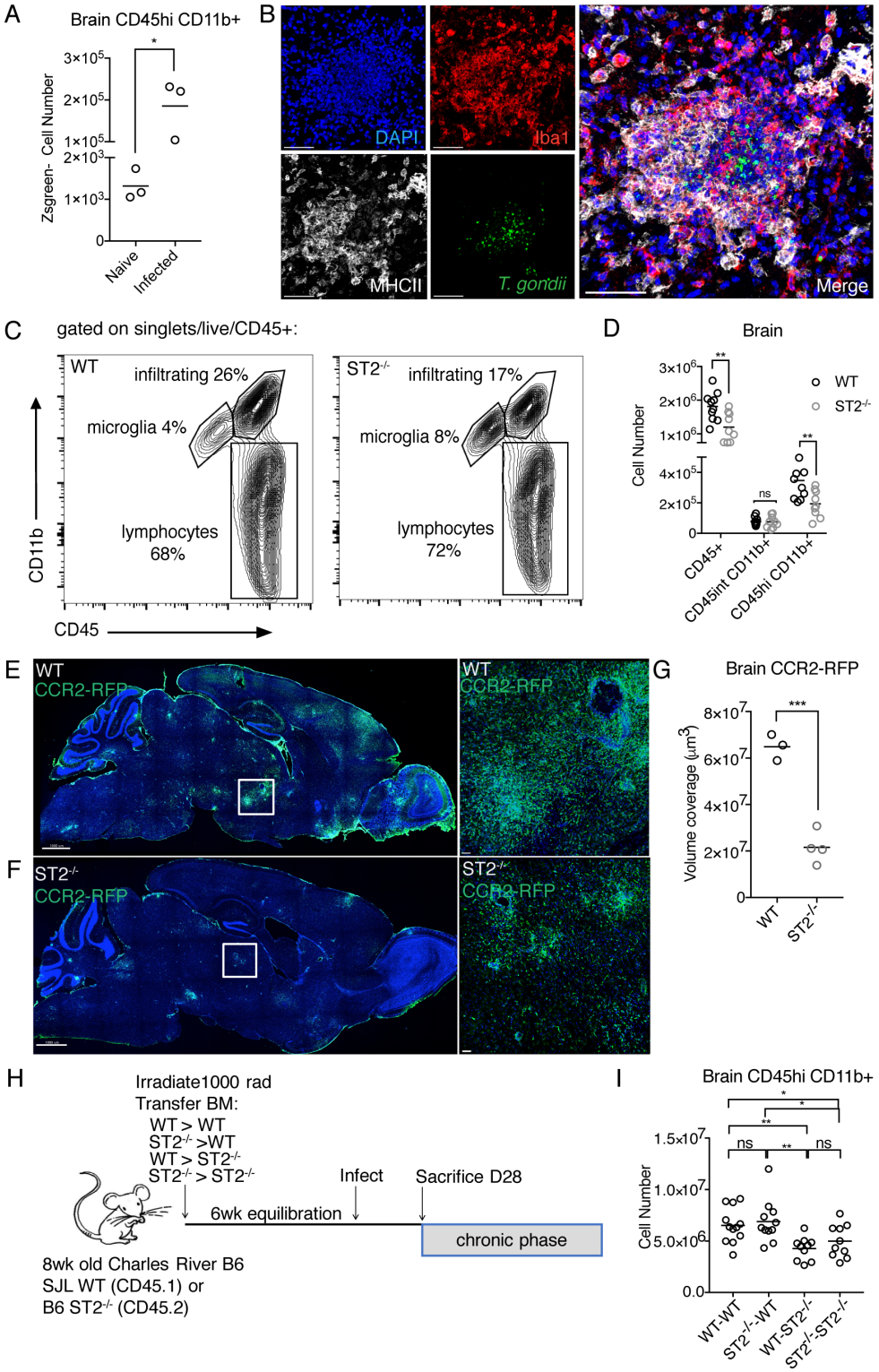

Figure 3. Trafficking of blood-derived myeloid cells to the *T. gondii*-infected brain is dependent on ST2 signaling on a radio-resistant responder

(A) Flow cytometry staining of brain mononuclear cells from naïve and chronically infected CX3CR1creERT2 Zsgreen microglia reporter mice. Zsgreen^{-} CD45^{hi}, CD11b^{+} (infiltrating myeloid) cell number was measured before and after infection, (n=3, Student's t-test, representative of 2 independent experiments)

(B) Immunofluorescence staining of an inflammatory focus in chronically infected wildtype mouse brain tissue for Iba1^{+} macrophages (red), MHCII^{+} cells (white), and *T. gondii* (green) – DAPI was used to detect nuclei (blue), scale bar = 50μm

(C) Representative flow cytometry plots measuring CD45 and CD11b expression in chronically infected wildtype and ST2$^{-/-}$ brains

(D) Flow cytometry measurement of total CD45^{+} immune cell number, CD45^{int} CD11b^{+} microglia number, and CD45^{hi} CD11b^{+} infiltrating myeloid number in chronically infected WT and ST2$^{-/-}$ brains, (n=3-4 per group, data was pooled from 3 experiments and analyzed by randomized block ANOVA).

(E-F) Representative tile scans of chronically infected wildtype and ST2$^{-/-}$ CCR2-RFP reporter mice. Sagittal brain slices were stained for RFP and DAPI staining was used to detect nuclei (blue), scale bar = 2000 μm, inset scale bar = 50μm

(G) Quantification of (E and F) by volume coverage of CCR2-RFP in sagittal brain sections using Imaris software, (n=3-4 per group, Student's t-test. Data points are representative of 3 averaged brain sections per mouse, performed once)

(H) Bone marrow chimera schematic – wildtype and ST2$^{-/-}$ mice were lethally irradiated and reconstituted with either wildtype or ST2$^{-/-}$ bone marrow. Mice were given six weeks for bone marrow to reconstitute prior to infection. Mice were sacrificed at 28 dpi and infiltrating myeloid cell numbers were assessed by flow cytometry.

(I) Flow cytometry measurement of CD45^{hi} CD11b^{+} infiltrating myeloid number in chronically infected chimera groups (n=5-6 per group, data was pooled from 2 experiments to demonstrate variability by infection and analyzed by randomized block ANOVA)

595 ns=p>0.05, *=p<0.05, **=p<0.01, ***=p<0.001

596 See also Figure S3.

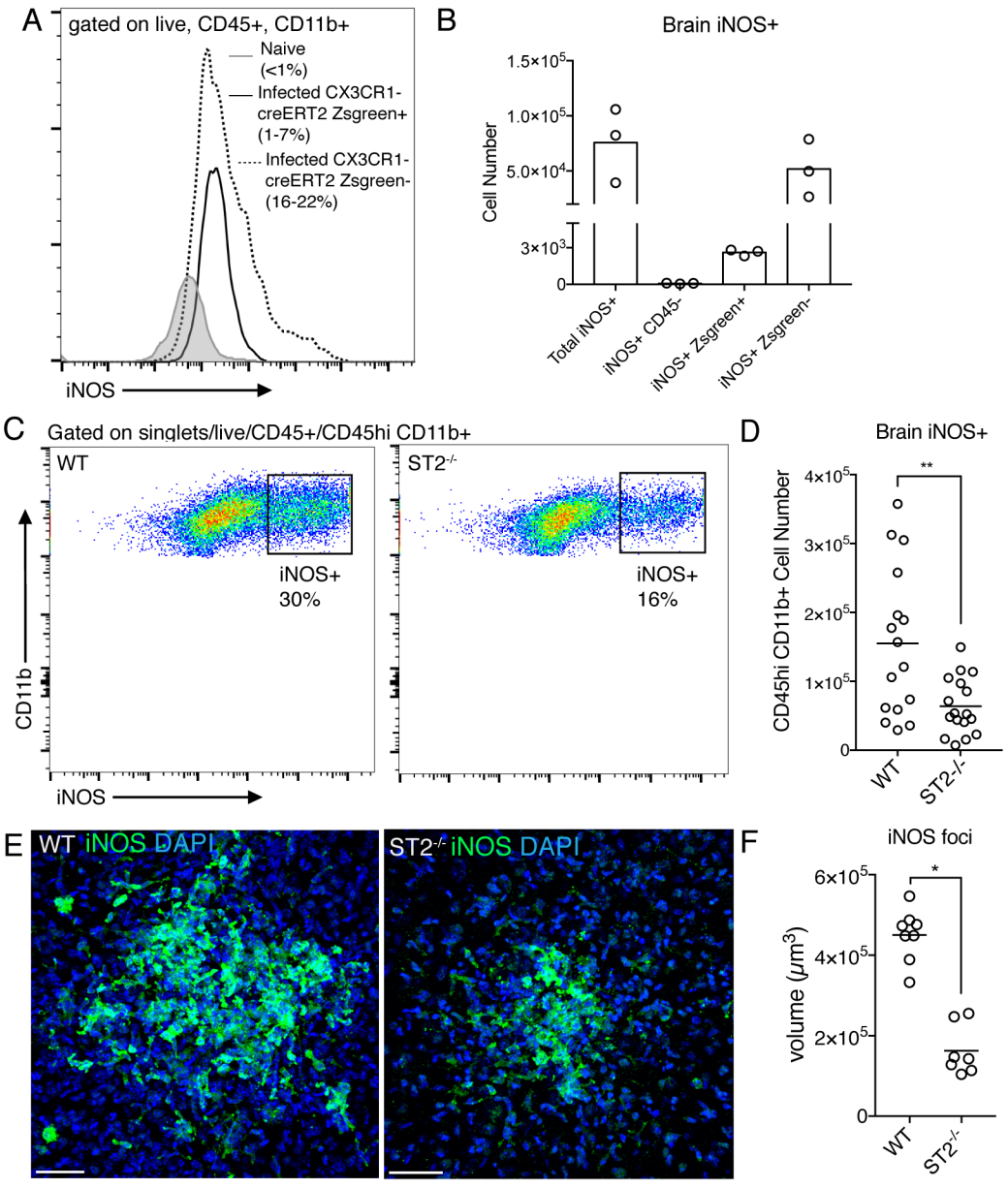

Figure 4. IL-33-ST2 signaling is required for engrafted myeloid cell-derived iNOS

(A) Representative flow cytometry histogram demonstrating iNOS expression in naïve and chronically infected CX3CR1-creERT2 ZsGreen microglia reporter mice. Microglia are ZsGreen^{+} and brain-infiltrating CD45^{hi} CD11b^{+} cells are ZsGreen-negative. (n=3, representative of 2 independent experiments)

(B) Flow cytometry measurement of $iNOS^+$ cells in brains of chronically infected CX3CR1-creERT2 ZsGreen microglia reporter mice. ZsGreen- cells are $CD45^{hi}$ $CD11b^+$ myeloid cells. (n=3, representative of 2 independent experiments).

(C) Representative flow cytometry dot plots measuring $iNOS^+$ frequency of $CD45^{hi}$ $CD11b^+$ brain-infiltrating cells in chronically infected wildtype and $ST2^{-/-}$ mice

(D) Flow cytometry measurement of brain infiltrating $CD45^{hi}$ $CD11b^+$ $iNOS^+$ cell number in chronically infected wildtype and $ST2^{-/-}$ mice (n=3-4 per group, data was pooled from 5 experiments and analyzed by randomized block ANOVA)

(E) Representative immunofluorescence staining in brain inflammatory foci for iNOS (green) between wildtype and $ST2^{-/-}$ mice, DAPI was used to detect nuclei (blue), scale bar = 50μm

(F) Quantification of (E) by iNOS foci voxels in sagittal brain sections of wildtype and $ST2^{-/-}$ infected mice using Imaris software, (n=4-5 per group, each data point represents an average of 3 sagittal sections, data was pooled from 2 experiments and analyzed by randomized block ANOVA) ns=p>0.05, *=p<0.05, **=p<0.01, ***=p<0.001

See also Figure S4.

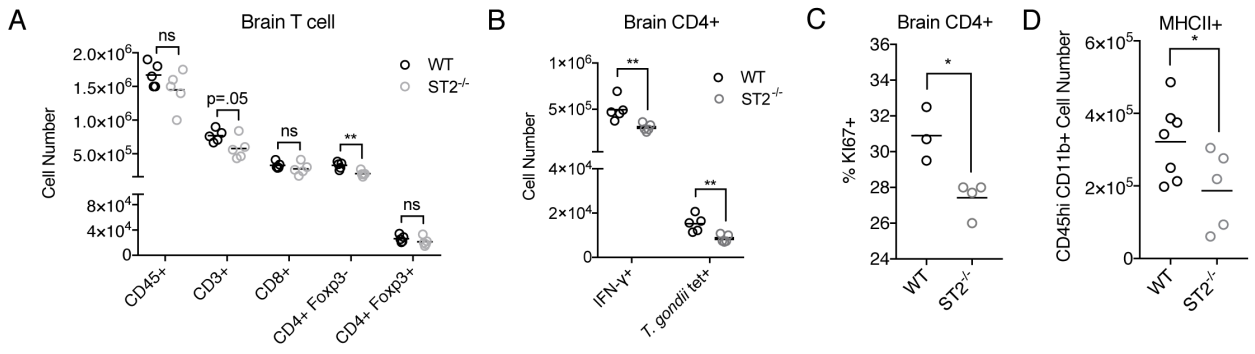

Figure 5. ST2$^{-/-}$ mice have deficient CD4^{+} T cell responses

(A) Flow cytometry measurement of T cell subsets, including total CD45^{+} immune cells, total CD3^{+} T cells, CD8^{+} T cells, CD4^{+} Foxp3^{-} effectors, and CD4^{+} Foxp3^{+} regulatory T cells from chronically infected wildtype and ST2$^{-/-}$ brains (n=5 per group, Student's t-test, representative of 5 independent experiments)

(B) Flow cytometry measurement of activated CD4^{+} T cells which were producing IFN-γ or were specific for a *T. gondii*-MHCII tetramer from chronically infected mice. Wildtype and ST2$^{-/-}$ brain mononuclear cells were stimulated with PMA/ionomycin for 5h (n=5 per group, Student's t-test, representative of 5 independent experiments)

(C) Flow cytometry measurement of Ki67^{+} frequency of brain CD4^{+} T cells from chronically infected wildtype and ST2$^{-/-}$ mice (n=3-4 mice per group, Student's t-test, performed once)

(D) Flow cytometry measurement of brain-infiltrating CD45^{hi} CD11b^{+} MHCII^{+} myeloid cell number in chronically infected wildtype and ST2$^{-/-}$ brains (n=3-4 per group, data was pooled from 2 experiments and analyzed by randomized block ANOVA)

ns=p>0.05, *=p<0.05, **=p<0.01, ***=p<0.001

See also Figure S5.

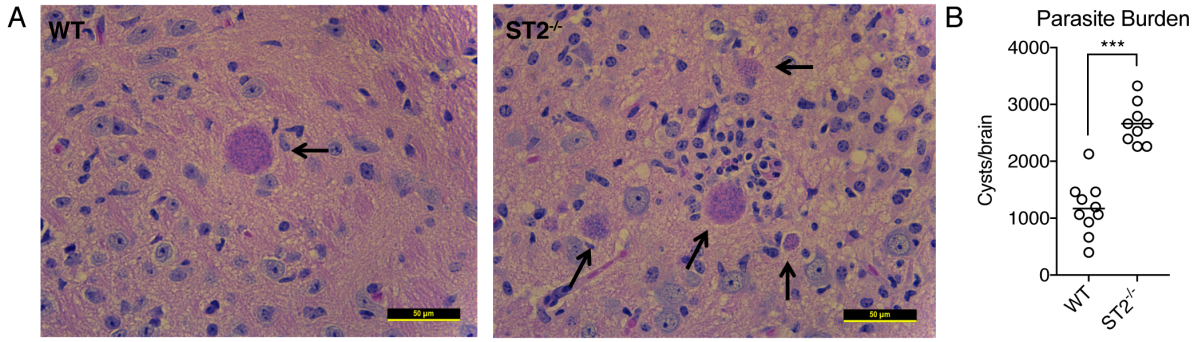

Figure 6. IL-33-ST2 signaling is required for control of brain parasite burden

(A) Hematoxylin and eosin staining of chronically infected brain tissue of wildtype and ST2$^{-/-}$ mice, arrows denote cysts, scale bar = 50μm

(B) Quantification of parasite burden by brain homogenate counts (n=3-4 per group, data was pooled from 3 experiments and analyzed by randomized block ANOVA) ns=p>0.05, *=p<0.05, **=p<0.01, ***=p<0.001

METHODS

Contact for reagent and resource sharing

Further information and requests for resources and reagents should be directed to and will be fulfilled by the Lead Contact, Tajie Harris (tajieharris@virginia.edu).

Experimental model and subject details

C57BL/6, CCL2-RFP^{flox}, CCR2^{RFP}, Ai6, and CX3CR1-CreERT2 mice were purchased from Jackson Laboratories. B6.SJL-Ptprc^{a} Pepc^{b}/BoyCrCl (C57BL/6 Ly5.1) mice were purchased from Charles River. ST2$^{-/-}$ mice were generously provided by Andrew McKenzie (Cambridge University). Ordering information for all strains is listed in the key resources table. Animals were housed in a UVA specific pathogen-free facility with a 12h light/dark cycle. Mice were age and sex matched for each experiment and were sacrificed in parallel. Animals were infected with *T. gondii* at 7 to 9 weeks of age and were housed separately from breeding animals. All procedures adhered to regulations of the Institutional Animal Care and Use Committee (ACUC) at the University of Virginia.

Human Brain tissue

Healthy and toxoplasmic encephalitis human brain samples from adult patients were obtained from the UVA Human Biorepository and Tissue Research Facility. Samples were preserved on paraffin embedded slides. Patient identification and medical background were withheld and therefore IRB approval was not required.

Parasite Strains

The avirulent, type II *Toxoplasma gondii* strain Me49 was used for all infections. *T. gondii* cysts were maintained in chronically infected (1-6 months) Swiss Webster (Charles River) mice. To generate cysts for experimental infections, CBA/J (Jackson Laboratories) mice were infected with

10 cysts from brain homogenate of Swiss Webster mice by i.p. injection in 200µl PBS. Cysts from 4 week-infected CBA/J brain homogenate were then used to infect animals in all experiments.

Immunohistochemistry

Mouse Tissue Immunofluorescence:

Reporter mice were perfused with 30 mL PBS followed by 30 mL 4% PFA (Electron Microscopy Sciences). All non-reporter strains were not perfused with PFA. Brains were cut along the midline and post-fixed in 4% PFA for 24h at 4°C. Brains were then cryoprotected in 30% sucrose (Sigma) for 24h at 4°C, embedded in OCT (Tissue Tek), and frozen on dry ice. Samples were then stored at -20°C. 40 µm sections were cut using a CM 1950 cryostat (Leica) and placed into a 24-well plate containing PBS. Sections were blocked in PBS containing 2% goat or donkey serum (Jackson ImmunoResearch), 0.1% triton, 0.05% Tween 20, and 1% BSA for 1h at RT. Sections were then incubated with primary antibody diluted in blocking buffer at 4°C overnight. Sections were washed the following day and incubated with secondary antibody in blocking buffer at room temperature for 1h. Sections were then washed and incubated with DAPI (Thermo Scientific) for 5 min at RT. Sections were then mounted onto Superfrost microscope slides (Fisherbrand) with aquamount (Lerner Laboratories) and coverslipped (Fisherbrand). Slides were stored at 4°C before use. Images were captured using an TCS SP8 confocal microscope (Leica) and analyzed using Imaris (Bitplane) software. Volumetric analysis was achieved using the surfaces feature of Imaris.

Human tissue Immunofluorescence:

Slides containing 4 µm sections of human brain tissue were received from the UVA Biorepository and Tissue Research Facility and de-paraffinized in a gradient from 100% xylene (Fisher) to 50% ethanol (Decon Laboratories). Slides were then washed in running water and distilled water.

Antigen retrieval was performed by incubating slides in antigen retrieval buffer (10 mM sodium citrate, .05%Tween-20, pH 6.0) in an Aroma digital rice cooker for 45 min at 95°C. Slides were then washed in running water followed by PBS-TW. Slides were then incubated with primary and secondary antibodies as described above for mouse brain tissue. Prior to imaging, Autoflourescence Eliminator Reagent was applied per the manufacturer's instructions (EMD Millipore).

Hematoxylin and Eosin Staining:

Brain tissue was fixed in 10% formalin and hematoxylin and eosin staining was performed by the UVA Research Histology Core. Images were acquired on a Brightfield DM 2000 LED microscope (Leica).

Tissue processing and flow cytometry

PBS-perfused whole brains were collected in 4 mL of complete RPMI (cRPMI)(10% fetal bovine serum, 1% NEAA, 1% pen/strep, 1% sodium pyruvate, 0.1% β-mercaptoethanol). Papain digestion was performed for the chimera experiment. To perform papain digestion, brains were cut into 6 pieces and incubated in 5 mL HBSS containing 50U/mL DNase (Roche), and 4U/mL papain (Worthington-Biochem) for 45 min at 37°C. Tissue was triturated first with a large bore glass pipette tip, and twice with a small-bore pipette tip every 15 min. In all other experiments collagenase/dispase was used to digest brain tissue. To perform collagenase/dispase digestion, perfused brains were minced using a razor blade and passed through an 18-gauge needle. Brains were then digested with 0.227mg/mL collagenase/dispase and 50U/mL DNase (Roche) for 1h at 37°C. Following digestion, homogenate was strained through a 70 μm nylon filter (Corning). Samples were then pelleted and spun in 20 mL 40% Percoll at 650g for 25 min. Myelin was aspirated and cell pellets were washed with cRPMI. Finally, cells were resuspended in cRPMI

and cells were enumerated. Spleens were collected into 4 mL cRPMI and macerated through a 40 µM nylon filter (Corning). Samples were pelleted and resuspended in 2 mL RBC lysis buffer (0.16 M NH_4Cl) Samples were then washed with cRPMI and resuspended for counting and staining. In cases of acute infection, 4mL of peritoneal lavage fluid was pelleted and resuspended in 2mL of cRPMI for counting and staining. Single cell suspensions were pipetted into a 96 well plate and pelleted. Samples were resuspended in 50 µL Fc Block (1 µg/ml 2.4G2 Ab (BioXCell), 0.1% rat gamma globulin (Jackson Immunoresearch)) for 10 min. Cells were then surface stained in 50 µL FACS buffer (PBS, 0.2% BSA, and 2 mM EDTA) for 30 min at 4°C. Following surface staining, cells were fixed for at least 30 min at 4°C with a fixation/permeabilization kit (eBioscience) and permeabilized (eBioscience). Samples were then incubated with intracellular antibodies in permeabilization buffer for 30 min at 4°C. Samples were run on a Gallios flow cytometer (Beckman Coulter), and analyzed using Flowjo software, v. 10.

qRT-PCR

Perfused brain tissue (100 mg) was placed into bead beating tubes (Sarstedt) containing 1mL Trizol reagent (Ambion) and zirconia/silica beads (Biospec). Tissue was homogenized for 30 seconds with a Mini-bead beater (Biospec) machine. RNA was extracted following homogenization per the Trizol Reagent manufacturer's instructions. Complementary DNA was then synthesized using a High Capacity Reverse Transcription Kit (Applied Biosystems). Taqman gene expression assays were acquired from Applied Biosystems and are listed in the key resources table. A 2X Taq-based mastermix (Bioline) was used for all reactions and run on a CFX384 Real-Time System (Bio-Rad). *Hprt* was used as the brain housekeeping gene and relative expression to wildtype controls was calculated as $2^{(-\Delta\Delta CT)}$.

***T. gondii* cyst counts**

Brain tissue (100 mg) was minced with a razor in 2mL cRPMI. Brain tissue was then passed through an 18-gauge and 22-gauge needle. 30 μL of resulting homogenate was pipetted onto a microscope slide (VWR) and counted on a Brightfield DM 2000 LED microscope (Leica). Cyst counts were extrapolated for whole brains.

Bone marrow chimera

Wildtype B6.SJL-Ptprc^{a} Pepc^{b}/BoyJ (C57BL/6 CD45.1) and ST2KO C57BL/6 mice were irradiated with 1000 rad. Irradiated mice received 3x10^{6} bone marrow cells from CD45.1 and CD45.2 donors the same day. Bone marrow was transferred by retro-orbital i.v. injection under isoflurane anesthetization. All mice received sulfa-antibiotic water for 2 weeks post-irradiation and were given 6 weeks for bone marrow to reconstitute. At 6 weeks, tail blood was collected from representative mice and assessed for reconstitution by flow cytometry. Mice were then infected for 4 weeks prior to analysis.

Statistical analyses

Statistical analyses comparing two groups at one time point were done using a Student's t-test in Prism software, v. 7.0a. In instances where data from multiple infections were combined to illustrate natural variation in virulence, a randomized block ANOVA was performed using R v. 3.4.4 statistical software to account for variability across experimental days. Genotype was modeled as a fixed effect and experimental day as a random effect. P values are indicated as follows: ns=not significant p>.05, * p < .05, ** p < .01, *** p < .001. The number of mice per group, test used, and p values are denoted in each figure legend. Data was graphed using Prism software, v.7.0a.

SUPPLEMENTARY FIGURES

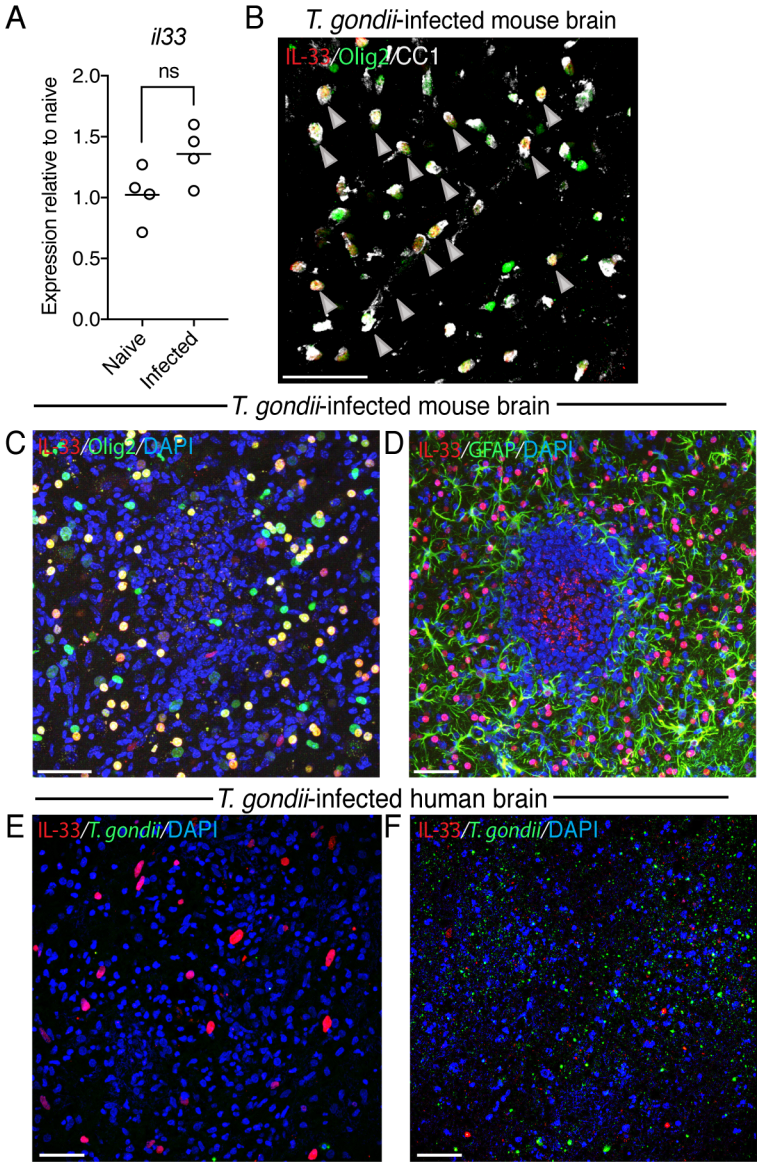

Figure S1. IL-33 expression during *T. gondii* infection of mouse and human brain tissue

(A) Quantitative real time PCR performed on whole brain homogenate of naïve and chronically infected wildtype mice for detection of *il33* transcript, (n=4 per group, Student's t-test, performed once) (B) Immunofluorescence staining for IL-33 (red), Olig2^{+} oligodendrocytes (green), and CC1^{+} mature oligodendrocyte marker (white) in brain tissue of chronically infected wildtype mice. Gray arrows denote co-localized CC1^{+} Olig2^{+} IL-33^{+} cells

(C-D) Representative images of loss of $Olig2^+$ oligodendrocytes (C) and $GFAP^+$ astrocytes (D) in inflammatory brain regions of chronically infected wildtype mice. Tissue sections were stained for IL-33 (red), Olig2 (green) (C), or IL-33 (red), $GFAP^+$ (green) (D) – DAPI was used to visualize nuclei (blue)

(E-F) Immunofluorescence staining of *T. gondii* infected human frontal cortex for intact IL-33 (red) in healthier-appearing regions with no *T. gondii* deposition (green) (E), and regions where *T. gondii* was present (F), scale bars = 50μm, ns=$p>0.05$, *=$p<0.05$, **=$p<0.01$, ***=$p<0.001$

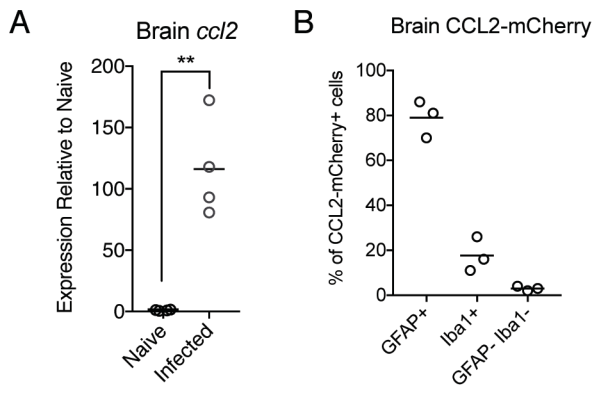

Figure S2. Characterization of brain CCL2 expression during *T. gondii* infection

(A) Quantitative real time PCR performed on whole brain homogenate of naïve and chronically infected wildtype mice for detection of *ccl2* transcript, (n=4 per group, Student's t-test, performed once) (B) Quantification of CCL2-mCherry^{+} cells by percentage of GFAP^{+} astrocytes, Iba1^{+} macrophages, and GFAP^{-} Iba1^{-} cells, (n=3 per group, data points represent an average percentage from approximately 300 cells per mouse, representative of 3 independent experiments)

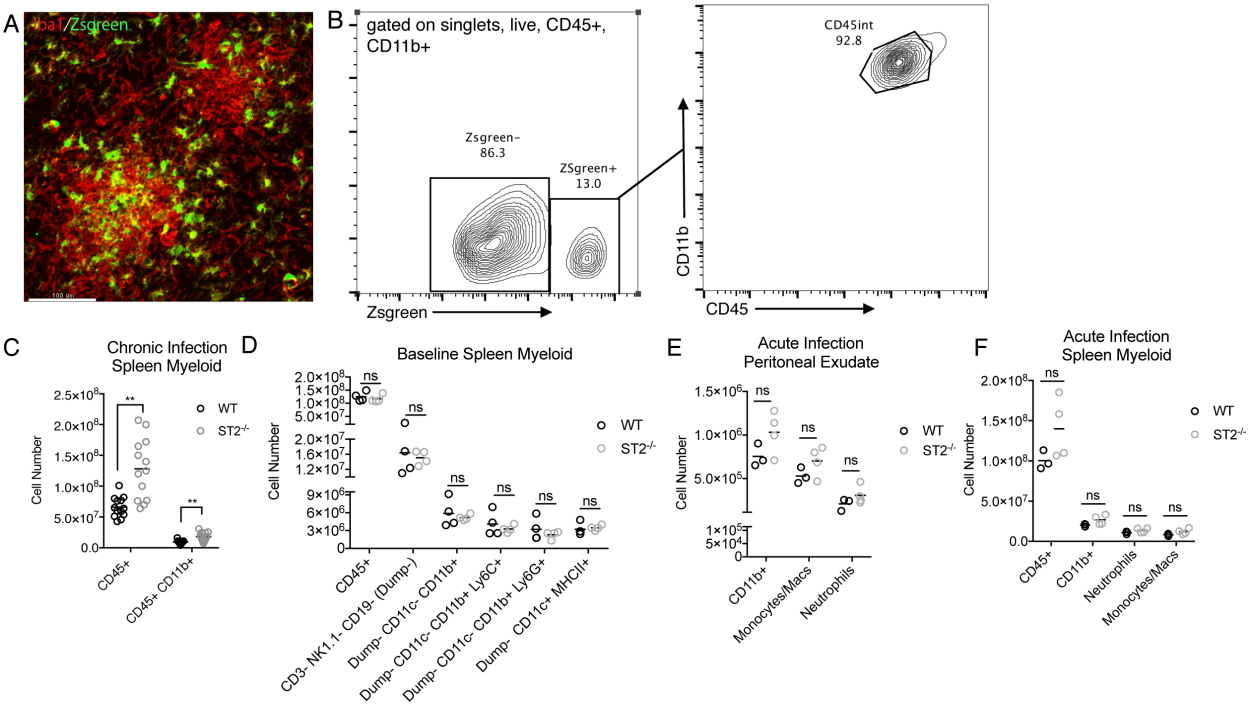

807

808 **Figure S3. Microglia reporter mice and peripheral myeloid cell responses to infection**

809 (A) Immunofluorescence of inflammatory foci in an infected CX3CR1-creERT2 x Ai6 (ZsGreen cre
810 reporter) mouse – microglia are co-labeled by Zsgreen fluorescence and the macrophage marker Iba1
811 (red), and peripherally-derived macrophages are Iba1^{+} Zsgreen^{-} scale bar = 100μm

812 (B) Frequency of Zsgreen^{+} microglia which remain CD45^{int} during chronic infection in a wildtype mouse
813 by flow cytometry

814 (C) Flow cytometry measurement of CD45^{+} CD11b^{+} cells from chronically infected wildtype and
815 ST2$^{-/-}$ spleens (n=3-4 per group, data was pooled from 5 experiments analyzed by randomized
816 block ANOVA)

817 (D) Flow cytometry measurement of myeloid cell subsets in uninfected wildtype and ST2$^{-/-}$ spleens
818 (n=4 per group, Student's t-test, representative of 2 independent experiments)

819 (E) Flow cytometry measurement of total CD11b^{+} myeloid cells, Ly6C^{+} monocytes and
820 macrophages, and Ly6G^{+} neutrophils from peritoneal lavage fluid of wildtype and ST2$^{-/-}$ mice
821 infected for 9 days, n=3-4 per group, Student's t-test, representative of 2 independent
822 experiments)

(F) Flow cytometry measurement of total $CD45^+$ immune cells, total $CD11b^+$ myeloid cells, $Ly6C^+$ monocytes and macrophages, and $Ly6G^+$ neutrophils from spleens of acutely infected (9 days) wildtype and $ST2^{-/-}$ mice, n=3-4 per group, Student's t-test, representative of 2 independent experiments) ns=p>0.05, *=p<0.05, **=p<0.01, ***=p<0.001

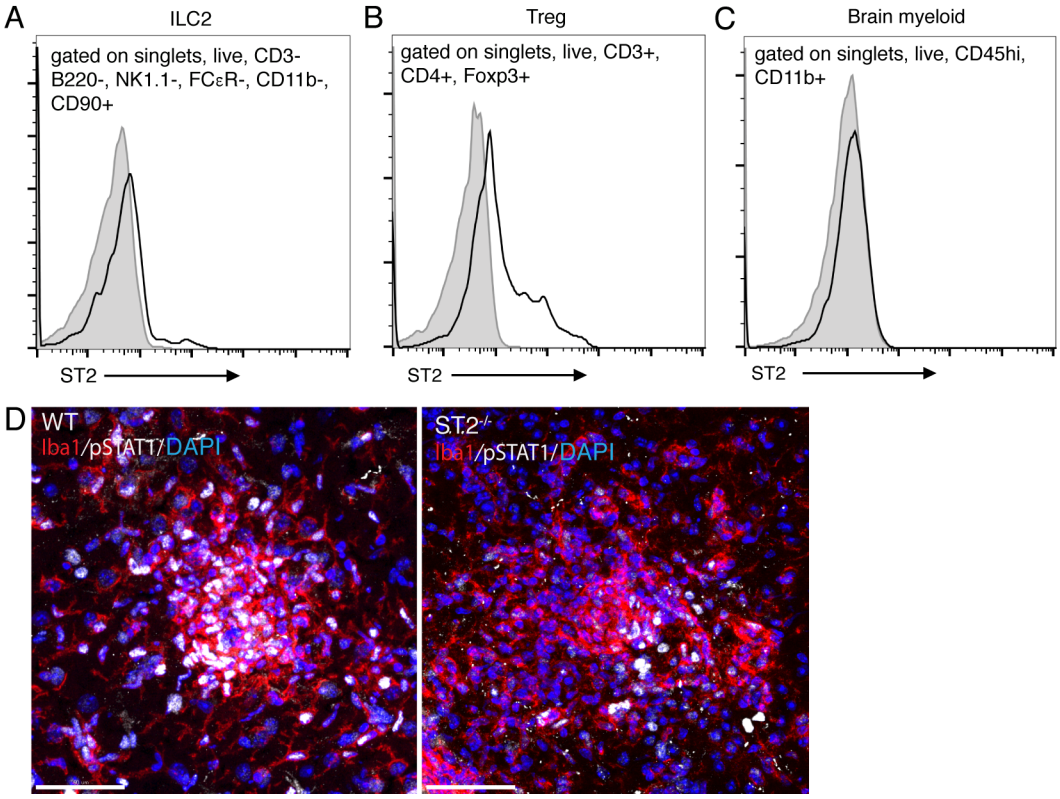

Figure S4. ST2 expression and phosphorylated-STAT1 levels in the CNS during chronic *T. gondii* infection

(A-B) Representative flow cytometry histograms demonstrating ST2 expression on type 2 innate lymphoid cells (A) and regulatory T cells (B) from brains of chronically infected wildtype mice (n=2, representative of 2 independent experiments)

(C) Representative flow cytometry histograms demonstrating lack of ST2 expression on $CD45^{hi}$ $CD11b^{+}$ infiltrating myeloid cells derived from brains of wildtype chronically infected mice, (n=2, representative of 2 independent experiments)

(D) Representative immunofluorescence of inflammatory foci in brains of chronically infected wildtype and $ST2^{-/-}$ mice, stained for $Iba1^{+}$ clustered macrophages (red) and pSTAT1 (white), DAPI was used to detect nuclei (blue), scale bar = 50 μm

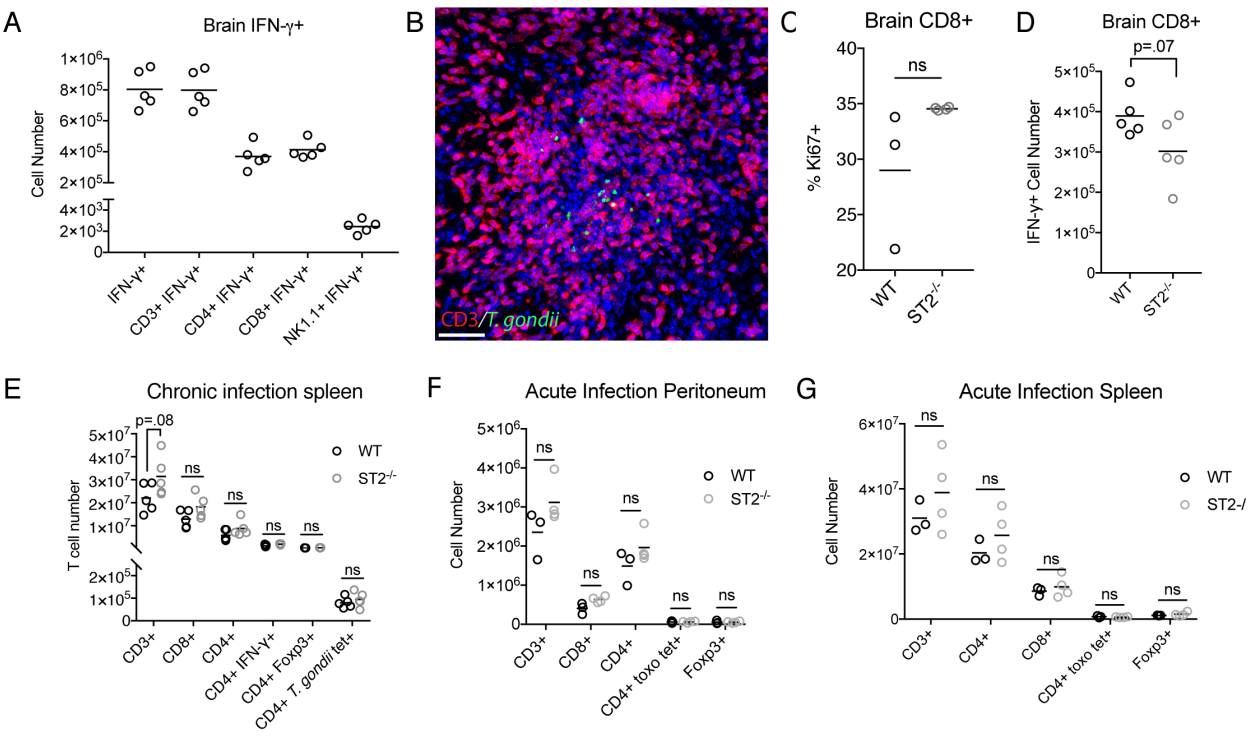

Figure S5. Characterization of T cell responses in wildtype and ST2$^{-/-}$ mice during acute and chronic *T. gondii* infection

(A) Flow cytometry measurement of IFN-γ^{+} CD3^{+} T cells and NK1.1^{+} NK cells from chronically infected brains of wildtype and ST2$^{-/-}$ mice, (n=5 per group, CD3 subsets are representative of 3 independent experiments, and NK cell subset was performed once)

(B) Immunofluorescence staining of reactivated *T. gondii* (green) surrounded by CD3^{+} T cells (red) from a brain of a chronically infected wildtype mouse, scale bar = 50μm

(C) Flow cytometry measurement of Ki67^{+} frequency of brain CD8^{+} T cells from chronically infected wildtype and ST2$^{-/-}$ mice (n=3-4 mice per group, Student's t-test, performed once)

(D) Flow cytometry measurement of CD8^{+} IFN-γ^{+} cell number from brains of chronically infected wildtype and ST2$^{-/-}$ mice, (n=3-4 per group, Student's t-test, representative of 3 independent experiments)

(E) Flow cytometry measurement of $CD3^+$ T cell subsets from chronically infected wildtype and $ST2^{-/-}$ spleens (n=5 per group, Student's t-test, representative of 3 independent experiments)

(F) Flow cytometry measurement of $CD3^+$ T cell subsets from peritoneal lavage fluid of wildtype and $ST2^{-/-}$ mice infected for 9 days, (n=3-4 per group, Student's t-test, representative of 2 independent experiments)

(G) Flow cytometry measurement of $CD3^+$ T cell subsets from acutely infected (9 days) wildtype and $ST2^{-/-}$ spleens, (n=3-4 per group, Student's t-test, representative of 2 independent experiments) ns=$p>0.05$, *=$p<0.05$, **=$p<0.01$, ***=$p<0.001$